Journal of Asian Ceramic Societies

Journal of Asian Ceramic Societies

journal homepage: www.elsevier.com/locate/jascer

Biomimetic mineralization of calcium phosphates in polymeric hydrogels containing carboxyl groups

Taishi Yokoi [a,*], Masakazu Kawashita [b], Chikara Ohtsuki [a]

[a] Department of Crystalline Materials Science, Graduate School of Engineering, Nagoya University, Furo-cho, Chikusa-ku, Nagoya 464-8603, Japan
[b] Department of Biomedical Engineering, Graduate School of Biomedical Engineering, Tohoku University, Aramaki-Aoba, Aoba-ku, Sendai 980-8579, Japan

ARTICLE INFO

Article history:
Received 16 January 2013
Received in revised form 23 April 2013
Accepted 23 April 2013
Available online 14 May 2013

Keywords:
Hydroxyapatite
Octacalcium phosphate
Hydrogel
Crystal growth
Carboxyl group

ABSTRACT

Biomimetic processing is an attractive method for the fabrication of inorganic crystalline materials with designed morphology under ambient conditions. Precipitation of inorganic solids in a hydrogel matrix could be regarded as mimicking the process of biomineralization and be called gel-mediated processing. The importance of the functional groups in reaction media and templates has been pointed out for such gel-mediated processing. In the present study, the role of carboxyl groups in hydrogel matrices on precipitation of calcium phosphate was investigated. Carboxyl groups in the hydrogel matrices provided pH buffering action, chelate formation with calcium ions and decreased the diffusion rate of calcium ions. The crystalline phase of the calcium phosphate changed from octacalcium phosphate to hydroxyapatite with increasing carboxyl group concentration in the hydrogels. The crystalline phase change is attributed to a decrease in the activation energy for calcium phosphate formation via a chelate structure involving calcium ions and carboxyl groups.

1. Introduction

Ceramic biomaterials are now widely used as bone substitutes in orthopedic applications. Sintered hydroxyapatite (HAp; $Ca_{10}(PO_4)_6(OH)_2$) is a typical example of bioactive ceramics, providing direct bonding to living bone. Because of its biological properties, synthesis of HAp and its related calcium phosphate compounds has become attractive. We have focused on synthetic routes of calcium phosphate compounds for the fabrication of designed microstructures, including compositions, phases, and the morphology of inorganic compounds. Development of biomimetic processing is an active research area for the fabrication of designed calcium phosphate crystals to produce well-designed materials through environmentally friendly processing. Organisms produce materials and structures with particular mechanical, optical and structural properties under standard temperature and pressure conditions [1]. We aim to develop novel materials and synthetic procedures using the materials synthesis mechanisms found in nature.

Calcium phosphate, especially HAp, can be formed on substrates by using a simulated body fluid (SBF) and its modified solutions [2–4]. SBF has been used to estimate the potential for the osteoconduction of materials [5]. The SBF is supersaturated with respect to HAp and is a metastable solution. Specific functional groups, for example COOH [6,7], SiOH [8] and TiOH [9], on material surfaces induce heterogeneous nucleation of calcium phosphate in the SBF and its modified solutions. These functional groups are negatively charged in the SBF and attract calcium ions. A type of chelate structure, composed of calcium ions and functional groups, induces heterogeneous nucleation. Calcium phosphate precipitates spontaneously in SBF, thus SBF can be used for biomimetic HAp coating on substrates. A technique mimicking biomineralization is generally conducted under conditions with a low degree of supersaturation, and hence the application of functional groups to control nucleation on material surfaces is useful for biomimetic HAp coating.

For further development of biomimetic fabrication, controlled precipitation of calcium phosphates in 3-dimensional network structures is expected to be important. Crystallization of calcium phosphates in a hydrogel matrix is regarded as a process that mimics biomineralization. Formation of poorly soluble compounds in hydrogel media is regarded as one crystal growth method.

* Corresponding author. Present address: Graduate School of Environmental Studies, Tohoku University, 6-6-20 Aoba, Aramaki, Aoba-ku, Sendai 980-8579, Japan. Tel.: +81 22 795 4274, fax: +81 22 795 4274.
E-mail addresses: yokoi@mail.kankyo.tohoku.ac.jp, yokoi.taishi@a.mbox.nagoya-u.ac.jp (T. Yokoi).

Peer review under responsibility of The Ceramic Society of Japan and the Korean Ceramic Society.

Production and hosting by Elsevier

2187-0764 © 2013 The Ceramic Society of Japan and the Korean Ceramic Society. Production and hosting by Elsevier B.V. All rights reserved.
http://dx.doi.org/10.1016/j.jascer.2013.04.003

Controlled formation of precipitates in hydrogels is called as gel-mediated processing, which is inspired from biomineralization. Calcium phosphate [10–17] and calcium carbonate [18–20] were reported as typical precipitates synthesized through gel-mediated processing. Formation of inorganic compounds by a mechanism that is similar to gel-mediated processing can be observed in nature. Biomineralization, such as the calcification in bones and shells, takes place in hydrogel-like environments. From the viewpoint of physical chemistry, calcification of bones can be regarded as the formation of HAp crystals in a collagen hydrogel. Hence, gel-mediated processing is categorized as a biomimetic process.

In biomimetic mineralization, the importance of functional groups in the hydrogel for calcium phosphate mineralization has been pointed out. Crystalline phases are affected by the degree of supersaturation in the calcium phosphate system [21]. The crystalline phases of calcium phosphate could be changed, depending on the functional groups present in the hydrogel matrix, because functional groups might change the degree of supersaturation required for nucleation. Crystalline phase control is an important issue in materials fabrication. To cite a specific case, synthesis of calcium phosphate-polymer composites through gel-mediated processing was studied to fabricate novel bone-repair materials [10,12]. Control of the crystalline phases of calcium phosphate is important in these materials, because they influence the biological and physicochemical properties of the composites. Understanding the roles of functional groups in a polymeric hydrogel matrix for calcium phosphate formation results in the fabrication of well-designed calcium phosphate-polymer composites. However the precise roles of the functional groups remain unclear. In this paper, the roles of functional groups, in particular COOH groups, on calcium phosphates formed in polymeric hydrogels were investigated. We focused on the COOH group, because this was expected to affect calcium phosphate formation, based on the results of SBF studies [22].

2. Experimental procedures

2.1. Chemicals

Acrylamide (Am, $CH_2CHCONH_2$, 98%) was purchased from Sigma–Aldrich Japan (Tokyo, Japan). Acrylic acid (Ac, $CH_2CHCOOH$, 98%), *N*,*N*′-methylenebisacrylamide (MBAAM, 99%), *N*,*N*,*N*′,*N*′-tetramethylethylenediamine (TEMED, 98%), diammonium hydrogen phosphate ($(NH_4)_2HPO_4$, 99%), ammonium peroxodisulfate ($(NH_4)_2S_2O_8$, 99%) and calcium nitrate tetrahydrate ($Ca(NO_3)_2{\cdot}4H_2O$, 98.5%) were purchased from Wako Pure Chemical Industries Ltd. (Osaka, Japan). Tris(hydroxymethyl)aminomethane (Tris, 99%) was purchased from Nacalai Tesque Inc. (Kyoto, Japan).

2.2. Preparation of polymeric hydrogels containing phosphate ions

Copolymer hydrogels composed of various mole fractions of Am and Ac were used as crystal growth matrices. Appropriate amounts of Am, Ac, MBAAM, TEMED and $(NH_4)_2HPO_4$ were dissolved in ultra-pure water. The pH values of the monomer solutions were adjusted to 7.9 by the addition of aqueous ammonia or nitric acid. The volume of the solution was adjusted in a volumetric flask. The final concentrations of chemicals in the solution were as follows: the sum of the concentrations of Am and Ac, 1.5 mol dm^{-3} (M); $(NH_4)_2HPO_4$, 0.20 M; MBAAM, 1.5×10^{-2} M; and TEMED, 3.0×10^{-2} M. The molar ratios of Am:Ac were 100:0, 75:25, 50:50, 25:75 and 0:100. A 20 cm^3 aliquot of the monomer solution was transferred to a glass vessel (capacity 50 cm^3, 5 cm in diameter). 9.0×10^{-5} mol of $(NH_4)_2S_2O_8$ was dissolved in the aliquot solution under vigorous stirring. After dissolution of $(NH_4)_2S_2O_8$, the glass vessel was covered with a poly(vinylidene chloride) film and a polyethylene lid to prevent water evaporation. Gelation was then allowed to take place at 60 °C for 24 h.

The initial pH values of the prepared gels were measured with a glass electrode-type pH meter (InLab® Solid; Mettler Toledo, Switzerland). The chemical structures of the prepared gels were characterized using a Fourier-transform infrared (FTIR) spectrometer (FT/IR-610; JASCO Co., Tokyo, Japan) using the KBr pellet method. The mass ratio of sample:KBr was 1:50. Each sample was scanned between 2000 and 1000 cm^{-1} at a resolution of 4 cm^{-1}. The gels were sliced and soaked in ultra-pure water for 1 h to remove chemicals contained within the hydrogels. This soaking operation was repeated three times. The rinsed gels were dried and the gels were then used for FTIR characterization.

2.3. Mineralization of calcium phosphate

Appropriate quantities of $Ca(NO_3)_2{\cdot}4H_2O$ and Tris were dissolved in ultra-pure water. The pH of the mixed solutions was adjusted to 7.0 by the addition of 1.0 M HCl solution. The volume of the solution was adjusted using a volumetric flask. The final concentrations of $Ca(NO_3)_2$ and Tris were fixed at 0.50 and 0.10 M, respectively. A 20 cm^3 volume of the $Ca(NO_3)_2$ solution was poured onto a synthesized polymeric hydrogel in a glass vessel. The vessel was covered with a poly(vinylidene chloride) film and a polyethylene lid, then maintained at 40 °C. After 1, 3, 5 or 10 days, the supernatant $Ca(NO_3)_2$ solutions on the polymeric hydrogels were removed and the gels were extracted from the glass vessels. The gels were cut in a vertical direction and the cross-section of each gel was then observed by the naked eye. The pH values of the removed solutions were measured with a glass electrode-type pH meter (D-51; Horiba Ltd., Japan). The concentrations of calcium and phosphate ions in the solutions were measured by inductively coupled plasma atomic emission spectroscopy (ICP-AES, Optima 2000DV, PerkinElmer Japan Co., Ltd., Japan).

The gels with precipitates were sliced and soaked in ultra-pure water for 1 h. This soaking operation was repeated three times. After the soaking operations, the sliced gels with precipitates were dried at 40 °C for 24 h. The dried samples were coated with thin gold films and then examined using scanning electron microscopy (SEM, JSM5600; JEOL Ltd., Japan). In addition, the dried samples were ground, and then the powdered samples were placed on glass sample holders for powder X-ray diffraction (XRD). The crystalline phases of the precipitates were identified by powder XRD (RINT 2100V; Rigaku Co., Tokyo, Japan) in the range $3^\circ \leq 2\theta \leq 40^\circ$ with a scan rate 1.0° min^{-1}, using CuKα radiation.

2.4. Measurement of the calcium ion adsorption capacity of the polymeric hydrogels

The polymeric hydrogels, synthesized from 1.0 cm^3 of monomer solution, without phosphate ions, were soaked in a 15 cm^3 volume of a 0.10 M $Ca(NO_3)_2$ solution. The pH values of the monomer solutions were adjusted to 7.0 using appropriate amounts of ammonia solution or nitric acid. The pH value of the $Ca(NO_3)_2$ solution was adjusted to 7.0 by the addition of Tris and HCl solution. The concentration of Tris in the $Ca(NO_3)_2$ solution was 1.0 mM. After 5 days, calcium ion concentrations in the solutions were measured by ICP-AES. The amounts of calcium ions adsorbed by the polymeric hydrogels were calculated from the decrease in the calcium ion

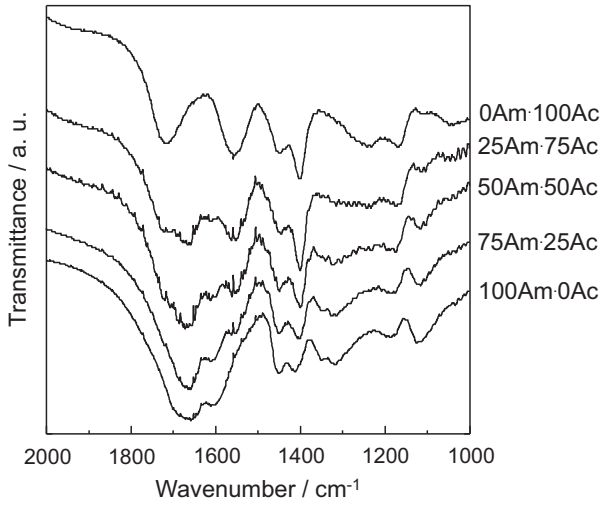

Fig. 1. Fourier-transform infrared (FTIR) spectra of 100Am·0Ac, 75Am·25Ac, 50Am·50Ac, 25Am·75Ac and 0Am·100Ac samples.

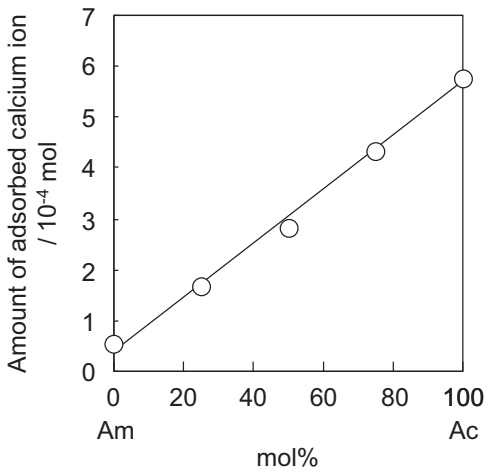

Fig. 2. Relationship between compositions of polymeric hydrogels and their calcium ion adsorption capacity.

concentration. This quantity was equated to the calcium adsorption capacity.

Hereafter, the prepared samples are denoted as *x*Am·*y*Ac. The notations Am and Ac denote acrylamide and acrylic acid, respectively, and *x* and *y* are the corresponding numerical values that give the ratio of components. For example, the notation 25Am·75Ac denotes that the polymeric hydrogel was synthesized from a monomer solution in which the molar ratio Am:Ac was 25:75.

3. Results

The initial pH values of the synthesized polymeric hydrogels containing $(NH_4)_2HPO_4$ were approximately 7.8. All the as-prepared gels were transparent and their appearance was similar, regardless of composition.

Fig. 1 shows the FTIR spectra of the samples. Absorption peaks were assigned based on previous reports [23,24]. The typical absorption peaks derived from COOH stretching mode of Ac and NH_2 deformation modes of Am were 1718 and 1609 cm^{-1}, respectively. The intensities of the absorption peak assigned to COOH increased with increasing Ac content in the gels. By contrast, the intensities of absorption peaks assigned to NH_2 concomitantly decreased. The other peaks were assigned as follows. The absorption peak detected at 1402 cm^{-1} was attributed to the C=C stretching mode of the vinyl group. The adsorption peak detected at 1453 cm^{-1} was attributed to the CH_2 bending mode and C—O—H in-plane deformation mode of COOH. The C—O stretching (amide I) vibration was detected at 1660 cm^{-1}.

Fig. 2 shows the relationship between the composition of the polymeric hydrogels and the amounts of calcium ions adsorbed by the gels. The quantity of adsorbed calcium ions increased linearly with increasing Ac content in the gels. The molar ratios between the amounts of calcium ions and COOH groups adsorbed (Ca^{2+}/COOH) in the 75Am·25Ac, 50Am·50Ac, 25Am·75Ac and 0Am·100Ac samples were 0.45, 0.38, 0.38 and 0.39, respectively.

Fig. 3 shows the reaction time dependence for the pH of the $Ca(NO_3)_2$ solutions in contact with the gels. The initial pH value of the $Ca(NO_3)_2$ solution was 7.0. After 1 day, the pH values were almost constant. At 10 days, the pH values for 100Am·0Ac, 75Am·25Ac, 50Am·50Ac, 25Am·75Ac and 0Am·100Ac were 4.1, 4.6, 5.1, 5.4 and 5.7, respectively. The decreases in pH values were found to decrease with increasing contents of Ac in the polymeric hydrogels.

Fig. 4 shows the reaction time dependence of the concentrations of calcium and phosphate ions in the $Ca(NO_3)_2$ solutions in contact with the gels. The initial calcium ion concentration was 500 mM. The calcium ion concentrations in all samples dramatically decreased over the course of day 1. The calcium ion concentrations at 1 day in 100Am·0Ac, 75Am·25Ac, 50Am·50Ac and 25Am·75Ac were 189, 205, 153 and 182 mM, respectively. The calcium ion concentrations in these samples gradually decreased with increasing reaction time. At day 10, the calcium ion concentrations in 100Am·0Ac, 75Am·25Ac, 50Am·50Ac and 25Am·75Ac decreased to 153, 97, 42 and 29 mM, respectively. The calcium ion concentration in 0Am·100Ac was almost constant at 22 mM from day 1 onwards. The initial phosphate ion concentration in the $Ca(NO_3)_2$ solution was 0 mM. The phosphate ion concentrations in the $Ca(NO_3)_2$ solutions in contact with the hydrogels were increased by the diffusion of phosphate ions from the hydrogels. In 100Am·0Ac, the phosphate ion concentration increased from 0 to 25 mM over the first day and then gradually increased. Finally, the

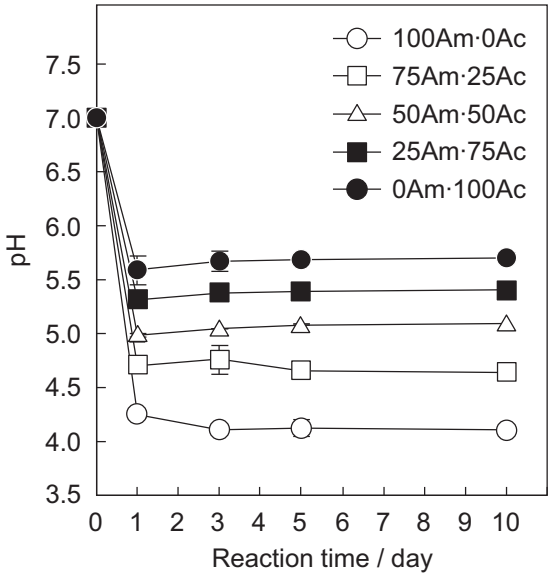

Fig. 3. Reaction time dependence of the pH of $Ca(NO_3)_2$ solutions in contact with 100Am·0Ac, 75Am·25Ac, 50Am·50Ac, 25Am·75Ac and 0Am·100Ac. The error bars indicate standard deviation.

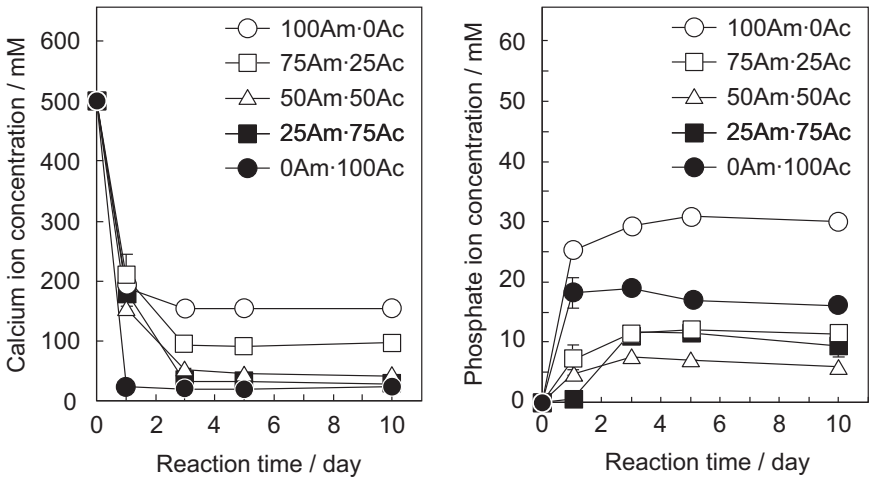

Fig. 4. Reaction time dependence of the concentrations of calcium and phosphate ions in $Ca(NO_3)_2$ solutions that were in contact with 100Am·0Ac, 75Am·25Ac, 50Am·50Ac, 25Am·75Ac and 0Am·100Ac samples. The error bars indicate standard deviation.

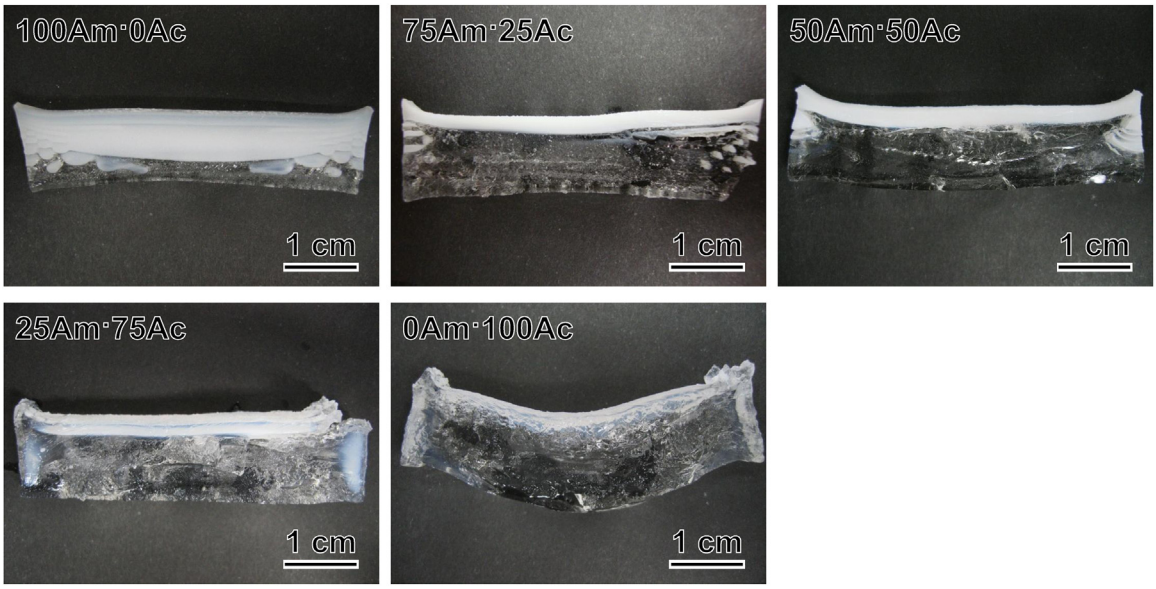

Fig. 5. Cross-sectional images of 100Am·0Ac, 75Am·25Ac, 50Am·50Ac, 25Am·75Ac and 0Am·100Ac. (The reaction time was 5 days.)

phosphate ion concentration was almost constant at 30 mM from day 5 onwards. The phosphate ion concentrations in 75Am·25Ac, 50Am·50Ac, 25Am·75Ac and 0Am·100Ac increased over the first 3 days. The phosphate ion concentrations in 75Am·25Ac, 50Am·50Ac, 25Am·75Ac and 0Am·100Ac were almost constant at 12, 7.0, 11 and 17 mM, respectively, from day 5 onwards.

Cross-sectional images of the samples are shown in Fig. 5. The reaction time for these samples was 5 days. Before calcification, the polymeric hydrogels were transparent. After calcification, white precipitates were observed. In the 100Am·0Ac, 75Am·25Ac and 50Am·50Ac samples, precipitates were observed in the gels. In the 25Am·75Ac and 0Am·100Ac samples, precipitates were observed on the surface of the gel. The semi-transparent parts were observed around the surface, namely around the interface between $Ca(NO_3)_2$ solution and the hydrogel, and these areas were hard.

Fig. 6 shows the powder XRD patterns of samples as a function of reaction time at 5 days. The diffraction peaks were assigned using the powder diffraction file database: the card numbers of HAp and OCP were #00-009-0432 and #01-074-1301, respectively. The

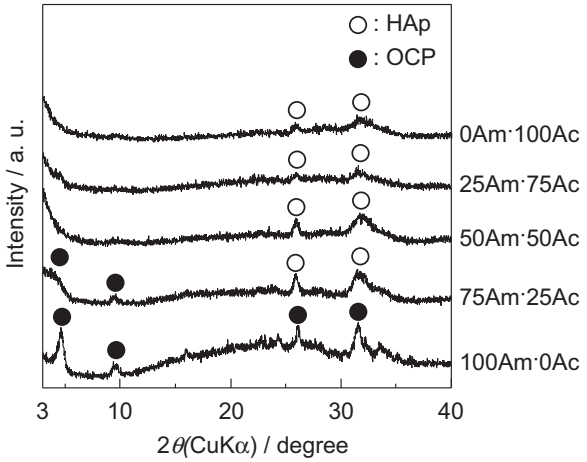

Fig. 6. Powder X-ray diffraction (XRD) patterns of 100Am·0Ac, 75Am·25Ac, 50Am·50Ac, 25Am·75Ac and 0Am·100Ac samples. (The reaction time was 5 days.)

Table 1
Reaction time dependence of crystalline phases of calcium phosphate formed in 100Am·0Ac, 75Am·25Ac, 50Am·50Ac, 25Am·75Ac and 0Am·100Ac samples. The diffraction peak intensities are shown by the following: strong +++; medium ++; weak +; and no specific peak –.

Sample	Reaction time/days			
	1	3	5	10
100Am·0Ac	OCP(+++)	OCP(+++)	OCP(+++)	OCP(+++)
75Am·25Ac	HAp(+++) OCP(+)	HAp(+++) OCP(+)	HAp(+++) OCP(+)	HAp(+++) OCP(+)
50Am·50Ac	HAp(+++)	HAp(+++)	HAp(+++)	HAp(+++)
25Am·75Ac	–	HAp(+)	HAp(++)	HAp(++)
0Am·100Ac	–	HAp(+)	HAp(++)	HAp(++)

strong peaks assigned to OCP were detected in the 100Am·0Ac sample. In the 75Am·25Ac sample, diffraction peaks assigned to OCP and HAp were detected. The intensities of the diffraction peaks assigned to OCP in the 75Am·25Ac sample were lower than that in the 100Am·0Ac sample. The diffraction peaks assigned to OCP were not detected and those assigned to HAp were detected in the 50Am·50Ac sample. The diffraction peaks assigned to HAp were detected in both 25Am·75Ac and 0Am·100Ac samples. The reaction time dependence of the crystalline phases of the samples is summarized in Table 1. The strong diffraction peaks assigned to OCP were detected in the 100Am·0Ac case at all reaction times. The strong diffraction peaks assigned to HAp and the weak diffraction peaks assigned to OCP were detected in the 75Am·25Ac sample at all reaction times. Similarly, the strong diffraction peaks assigned to HAp were detected in the 50Am·50Ac sample at all reaction times. In the 25Am·75Ac and 0Am·100Ac cases, a small amount of white precipitate near the surface of the gels was observed, but no diffraction peak was detected at day 1. The weak diffraction peaks assigned to HAp were detected in these samples at 3 days. The diffraction peaks assigned to HAp were detected in the 25Am·75Ac and 0Am·100Ac samples at both 5 and 10 days. The crystalline phases changed from OCP to HAp with increasing Ac content of the gels.

The morphologies of the precipitates are shown in Fig. 7. In the 100Am·0Ac, 75Am·25Ac and 50Am·50Ac samples, granule-shape precipitates with particles approximately 3 μm in diameter were observed in the gels. No precipitate was formed in the gels for the 25Am·75Ac and 0Am·100Ac samples. In these samples, precipitates were observed only at the surfaces of the gels. Granular particles with network-like structures were observed in the 25Am·75Ac sample. The particles were partially covered by polymeric gels. Granular precipitates with particles approximately 3 μm in diameter were observed at the surface of the 0Am·100Ac sample.

4. Discussion

The FTIR spectra (Fig. 1) and calcium ion adsorption capacity of gels (Fig. 2) imply that the compositions of the synthesized polymeric hydrogels were almost identical to those of the corresponding monomer solution. The intensities of absorption peaks due to the COOH group increased with increasing Ac content in the monomer solutions. Additionally, the intensities of absorption peaks derived from NH_2 decreased with decreasing Am content in the monomer solution. A previous report indicated that the binding molar ratio of (calcium ion):COOH in poly(acrylic acid) was approximately 1:3 [25]. The molar ratios between the amounts of adsorbed calcium ions and COOH groups in the 50Am·50Ac, 25Am·75Ac and 0Am·100Ac samples were 0.38, 0.38 and 0.39, respectively. These molar ratios of amounts of adsorbed calcium ions and COOH group were almost equal to 1/3 (0.33), and hence calcium ion adsorption was mainly caused by the COOH groups of Ac. In the 75Am·25Ac case, the molar ratio between the amounts of adsorbed calcium ions and COOH groups was 0.45, and this larger value was generated by calcium ion adsorption on the Am component. The results of FTIR characterization and measurement of the calcium ion adsorption capacity of the gels indicate that almost all Ac and Am in the monomer solutions were used for polymeric hydrogel formation. The absorption peak due to the vinyl group was detected by FTIR (Fig. 1). This absorption peak is considered to be due to unreacted MBAAM, because absorption peaks derived from the COOH stretching mode of Ac and NH_2 deformation mode of Am implied that Ac and Am in the monomer solutions were used for polymeric hydrogel formation. Additionally, the calcium ion adsorption capacity of the gels also implied that almost all Ac in the monomer solutions was used for polymeric hydrogel formation.

According to the data in Fig. 3, the pH values of the experimental systems were decreased by calcium phosphate formation. The crystalline phases of calcium phosphate formed in the samples were OCP and/or HAp (Fig. 6 and Table 1). When PO_4^{3-} and/or HPO_4^{2-} were consumed by the formation of OCP ($Ca_8(HPO_4)_2(PO_4)_4{\cdot}5H_2O$) and/or HAp ($Ca_{10}(PO_4)_6(OH)_2$), the following reaction occurred, and hence the pH of the reaction system decreased:

$$HPO_4^{2-} \rightarrow PO_4^{3-} + H^+$$

$$H_2PO_4^{-} \rightarrow HPO_4^{2-} + H^+ \quad (1)$$

The decreases in pH values of the samples with lower Ac contents were larger than those of the samples with higher Ac contents and this phenomenon was caused by an increase in pH buffering capacity with increasing Ac content. Carboxylic acids are widely used as pH buffers. In the polyacrylamide hydrogel with the succinic acid system, we reported that the magnitude of the decreases in pH values generated by OCP formation in the gels decreased with increasing succinic acid concentration [17]. In the reaction system, pH changes were buffered by the COOH group of succinic acid, and it is likewise considered that the pH changes in this experimental system were buffered by the Ac component. The amounts of precipitates are another factor causing pH differences, depending on the hydrogel composition. According to Fig. 5, the amounts of precipitates decreased with an increase in the Ac content of the gels. The likely reason for these phenomena is chelation of calcium ions by the COOH groups of Ac. The activity of calcium ions was decreased by complex formation, and hence the amount of the precipitate decreased with increasing Ac content in the sample. Hardening of the gels was observed, especially for the 25Am·75Ac and 0Am·100Ac samples, around their top surface. Gelation of poly(acrylic acid) due to cross-linking of COOH groups in the polymer by calcium ions is a well known phenomenon [26]. Hence the hardening of the gels was due to cross-linking of Ac components in the gels by calcium ions and this phenomenon showed that chelation of calcium ions was taking place. Hence, the magnitude of the decrease in pH by calcium phosphate formation shrank while increasing pH buffering capability with increasing Ac contents in the gels, as well as by decreases in the amount of calcium phosphate formed in the reaction systems through chelate formation.

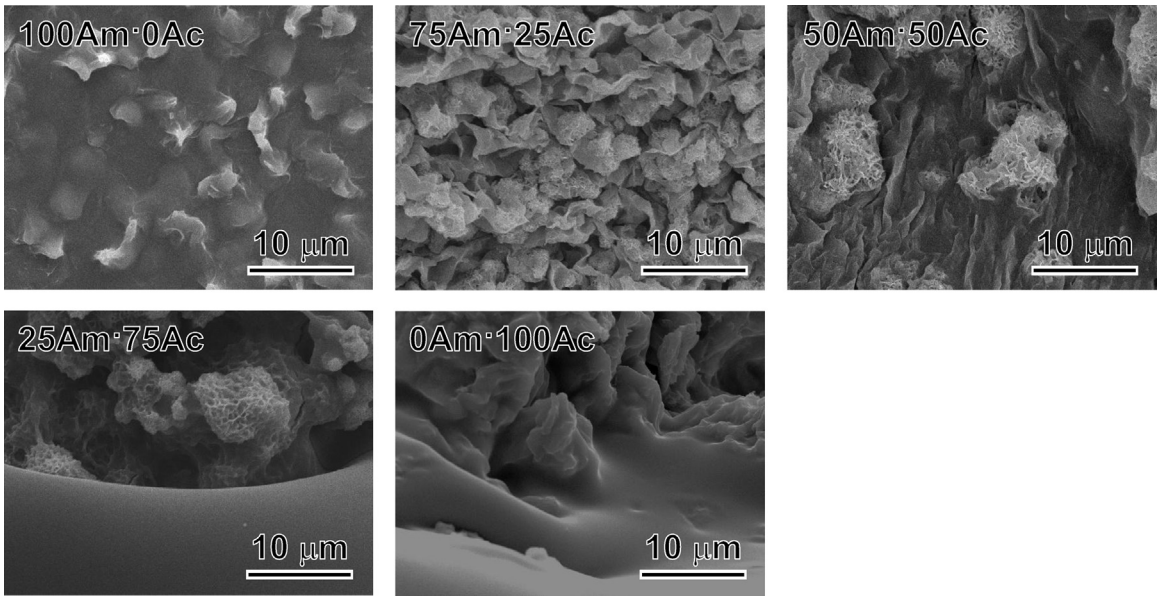

Fig. 7. Scanning electron microscope images of precipitates. In 100Am·0Ac, 75Am·25Ac and 50Am·50Ac, precipitates were formed in the gels. On the other hand, in 25Am·75Ac and 0Am·100Ac, precipitates were only observed near the surfaces of the gels.

Chelate formation controls the precipitation sites and the crystalline phases of calcium phosphates formed. In the case of 100Am·0Ac, calcium ions diffused into the hydrogel and granule-shape precipitates were formed inside the gel (Figs. 5 and 7). The thicknesses of the precipitation areas in the 75Am·25Ac and 50Am·50Ac samples were smaller than that in the 100Am·0Ac sample (Fig. 5). Granule-shape precipitates were observed in the precipitation areas of 75Am·25Ac and 50Am·50Ac. In 25Am·75Ac and 0Am·100Ac, granule-shape HAp was formed at the surface of the gels (Figs. 5 and 7). These findings imply that the COOH groups of the Ac component inhibited the diffusion of calcium ions into the gels from the $Ca(NO_3)_2$ solution in contact with the gels. The results observed are due to the chelation of calcium ions and a decrease in their diffusion rate caused by electrostatic interaction between Ca^{2+} and COO^- moieties.

The crystalline phases of precipitates were changed from OCP to HAp with increasing Ac content in the gels (Fig. 6 and Table 1). The initial pH values of the hydrogels and $Ca(NO_3)_2$ solution were 7.8 and 7.0, respectively. The initial pH conditions in the reaction systems were almost the same, regardless of hydrogel composition; hence pH is not the dominant factor for crystalline phases of calcium phosphate in these experimental conditions. It was reported that the crystalline phases of calcium phosphate precipitating in a solution depend on the supersaturation ratio of the crystalline phase of calcium phosphate [21]. For example, the order of supersaturation ratio, which is calculated for HAp, required for formation is amorphous calcium phosphate (ACP) > OCP > defective hydroxyapatite (DHAp) > HAp under conditions with pH 7. It was difficult to calculate a supersaturation ratio inside the gel, but it can be assumed that the supersaturation ratio inside is related to the supersaturation ratio of the $Ca(NO_3)_2$ solution in contact with a gel. The supersaturation ratio of HAp in the $Ca(NO_3)_2$ solution was calculated based on assumptions used in the previous paper [16]. Specifically, the pH values and the concentrations of calcium and phosphate ions in the gel were equal to those in the $Ca(NO_3)_2$ solution in contact with the gel. In the hydrogels, the activity coefficients of calcium and phosphate ions would be <1, because the polymer network of the hydrogels would decrease the activity of ions. A calculation method for the activity coefficient in hydrogels has not been established and measurement of the activity of calcium and phosphate ions in hydrogels is technically difficult. Hence, the activity coefficients of calcium and phosphate ions in hydrogels are regarded as 1 for descriptive purposes. With these assumptions, the supersaturation ratio of HAp (S(HAp)) was calculated using the following equation:

$$S(\mathrm{HAp}) = \mathrm{IAP}(\mathrm{HAp})/K\mathrm{sp}(\mathrm{HAp}) \quad (2)$$

In Eq. (2), IAP and Ksp are the ion activity product and the solubility product, respectively. IAP for HAp was calculated using Eq. (3), and the pKsp(HAp) value under these experiments was supposed to be 117.2, which was previously reported at 37 °C [27].

$$\mathrm{IAP(HAp)} = [Ca^{2+}]^{10}[PO_4{}^{3-}]^6[OH^-]^2 \quad (3)$$

Fig. 8 shows the reaction time dependence of S(HAp). The S(HAp) values were also constant at 5 days and longer. This finding indicates that the reaction systems had achieved steady state at 5 days and longer. The data for pH, calcium and phosphate ions concentrations and crystalline phases present also show that the reaction systems were at steady state at these reaction times.

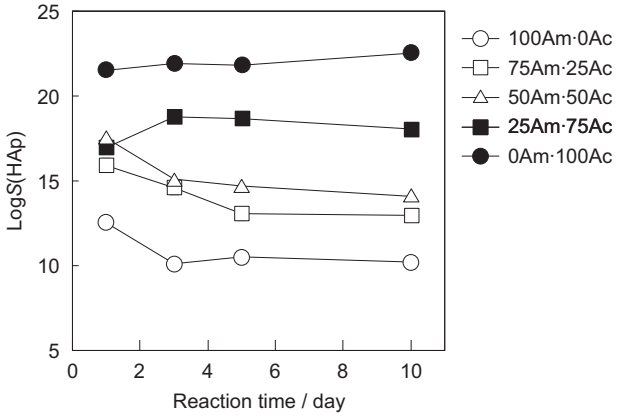

Fig. 8. Reaction time dependence of the supersaturation ratio of HAp (S(HAp)) in $Ca(NO_3)_2$ solutions that were in contact with 100Am·0Ac, 75Am·25Ac, 50Am·50Ac, 25Am·75Ac and 0Am·100Ac samples.

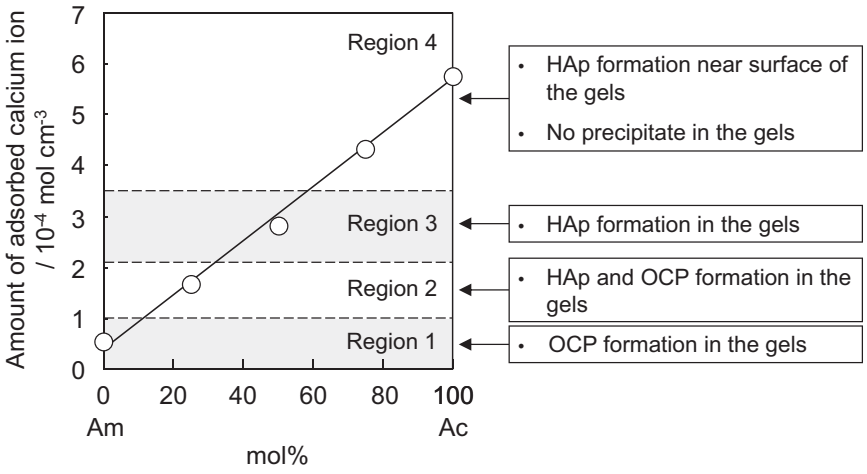

Fig. 9. Relationships between the compositions of polymeric hydrogels, the calcium ion adsorption capacity, crystalline phases of calcium phosphate and the formation area of calcium phosphates.

The pH values of the samples were almost constant after 1 day (Fig. 3). The calcium and phosphate ions concentrations were almost constant after 5 days (Fig. 4). No changes in crystalline phases and diffraction peak intensities were observed after 5 days (Table 1). The order of the *S*(HAp) values after 5 days was 0Am·100Ac > 25Am·75Ac > 50Am·50Ac > 75Am·25Ac > 100Am·0Ac. This order is equal to that considered for the pH value of the samples at steady state. The *S*(HAp) values increased with increasing pH values in the reaction systems. It is reasonable that the solubility of HAp decreases with increasing pH in the range 4–8 [28]. The pH values were determined by the composition of the gels, namely the Ac content in the gels. Hence, the *S*(HAp) values in regions of the gels where calcium phosphate formation occurs may be increased by increasing the Ac content in the gel. The order of *S*(HAp) assumed from *S*(HAp) values of $Ca(NO_3)_2$ solution was opposite to the *S*(HAp) values assumed from the crystalline phases of calcium phosphate. The order of *S*(HAp) required for formation is ACP > OCP > DHAp > HAp under conditions with pH 7 [21], and hence it should be considered that there is a decrease in the activation energy of nucleation of calcium phosphate by COOH groups. The functional groups present in acrylamide and acrylic acid are $CONH_2$ and COOH, respectively. The effects of $CONH_2$ on calcium phosphate formation can be neglected, because the activity of the $CONH_2$ group for induction of heterogeneous nucleation of calcium phosphate is very much weaker than the activity of the COOH in the SBF environment [22]. The cause of the induction of calcium phosphate nucleation is likely to be a chelate formation, involving calcium ions and COOH groups [22]. Hence, the nucleation process would be changed from homogeneous to heterogeneous nucleation with increasing Ac content in the gels. Generally, heterogeneous nucleation occurs preferentially over homogeneous nucleation, because of its smaller activation energy. Hence, we consider that the formation of the chelate structure of COOH groups and calcium ions decreases the activation energy for calcium phosphate nucleation. The *S*(HAp) estimated from pH, calcium and phosphate ions concentrations in the $Ca(NO_3)_2$ solution increased with increasing Ac content in the gels, but actually the supersaturation required for nucleation would be decreased by the COOH groups in the Ac component. Hence, HAp in the 50Am·50Ac, 25Am·75Ac and 0Am·100Ac samples was formed under low supersaturation conditions and OCP in the 100Am·0Ac case was formed under higher supersaturation conditions, although the degree of supersaturation was apparently low. The activation energy decreased with increasing Ac content in the gels, and hence both HAp and OCP were formed in the 25Am·75Ac sample. Estimation of the supersaturation ratio inside the gels from the supersaturation ratio of $Ca(NO_3)_2$ solutions contacted with the gels is important for understanding the mineralization process of calcium phosphates in the gels. Our results indicate that the decrease in the activation energy of nucleation by the functional groups in the hydrogel matrix must be considered.

Fig. 9 shows the relationships between the calcium ion adsorption capacity of the hydrogels per 1 cm^3 of hydrogel, the composition of the hydrogel and the crystalline phases of calcium phosphate observed. In Region 1, hydrogels did not contain COOH groups, and hence OCP was formed in the gels under high supersaturation conditions. In Region 3, the activation energy of nucleation of calcium phosphate was decreased by a chelate structure involving calcium ions and COOH groups, and hence HAp was formed in the gels under low supersaturation conditions. In Region 2, both HAp and OCP were formed in the gels, because Region 2 is a transition state between Regions 1 and 3. In Region 4, the COOH groups in the hydrogel chelate with calcium ions and inhibit the diffusion of calcium ions from the $Ca(NO_3)_2$ solution to the hydrogel, and hence HAp was formed near the surface of the hydrogels, with no precipitate being observed in the gels.

5. Conclusions

The roles of the COOH groups within the hydrogels in calcium phosphate formation through gel-mediated processing were: pH buffering action, chelate formation with calcium ions and decreasing the diffusion rate of calcium ions. Decreases in the pH values of the samples by calcium phosphate formation were found to be proportional with an increase in the concentration of the COOH groups in the gels by the pH-buffering action of the COOH groups. The crystalline phase of the calcium phosphate was changed from octacalcium phosphate to hydroxyapatite with increasing concentrations of COOH groups in the gels. The cause of the crystalline phase change is due to a decrease in the activation energy of calcium phosphate formation by forming a chelate structure involving calcium ions and COOH groups. The decrease in the diffusion rate of calcium ions was due to chelate formation and the electrostatic interactions between Ca^{2+} and COO^- entities. Hence, the thickness of the precipitation area gradually decreased with an increase in the concentration of COOH groups in the gels.

Conflict of interest statement

The authors declare that there is no conflict of interest.

Acknowledgment

This work was partially supported by a Grant-in-Aid for Scientific Research (No. 22107007) on the Innovative Areas of "Fusion Materials: Creative Development of Materials and Exploration of Their Function through Molecular Control" (No. 2206) from the Ministry of Education, Culture, Sports, Science and Technology, Japan (MEXT).

References

[1] S. Mann, Biomineralization, Oxford University Press, Oxford (2001).
[2] Y. Abe, T. Kokubo and T. Yamamuro, J. Mater. Sci. Mater. Med., 1, 233–238 (1990).
[3] A.C. Tas and S.B. Bhaduri, J. Mater. Res., 19, 2742–2749 (2004).
[4] C. Ohtsuki, M. Kamitakahara and T. Miyazaki, J. Tissue Eng. Regen. Med., 1, 33–38 (2007).
[5] C. Ohtsuki, T. Kokubo, K. Takatsuka and T. Yamamuro, Nippon Seramikusu Kyokai Gakujutsu Ronbunshi, 99, 1–6 (1991).
[6] T. Miyazaki, C. Ohtsuki, Y. Akioka, M. Tanihara, J. Nakao, Y. Sakaguchi and S. Konagaya, J. Mater. Sci. Mater. Med., 14, 569–574 (2003).
[7] T. Ichibouji, T. Miyazaki, E. Ishida, M. Ashizuka, A. Sugino, C. Ohtsuki and K. Kuramoto, J. Ceram. Soc. Jpn., 116, 74–78 (2008).
[8] P. Li, C. Ohtsuki, T. Kokubo, K. Nakanishi, N. Soga, T. Nakamura and T. Yamamuro, J. Am. Ceram. Soc., 75, 2094–2097 (1992).
[9] P. Li, C. Ohtsuki, T. Kokubo, K. Nakanishi, N. Soga and K. de Groot, J. Biomed. Mater. Res., 28, 7–15 (1994).
[10] K. Furuichi, Y. Oaki, H. Ichimiya, J. Komotori and H. Imai, Sci. Technol. Adv. Mater., 7, 219–225 (2006).
[11] S. Teng, J. Shi and L. Chen, Colloids Surf. B, 49, 87–92 (2006).
[12] R. Yoh, T. Matsumoto, J. Sasaki and T. Sohmura, J. Biomed. Mater. Res. A, 87, 222–228 (2008).
[13] K. Teshima, M. Sakurai, S. Lee, K. Yubuta, S. Ito, T. Suzuki, T. Shishido, M. Endo and S. Oishi, Cryst. Growth Des., 9, 650–652 (2009).
[14] T. Yokoi, M. Kawashita, G. Kawachi, K. Kikuta and C. Ohtsuki, J. Mater. Res., 24, 2154–2160 (2009).
[15] T. Yokoi, M. Kawashita, K. Kikuta and C. Ohtsuki, Mater. Sci. Eng. C, 30, 154–159 (2010).
[16] T. Yokoi, M. Kawashita, K. Kikuta and C. Ohtsuki, J. Cryst. Growth, 312, 2376–2382 (2010).
[17] T. Yokoi, H. Kato, M. Kamitakahara, M. Kawashita and C. Ohtsuki, J. Ceram. Soc. Jpn., 118, 491–497 (2010).
[18] O. Grassmann and P. Löbmann, Chem. Eur. J., 9, 1310–1316 (2003).
[19] O. Grassmann and P. Löbmann, Biomaterials, 25, 277–282 (2004).
[20] Y. Oaki, S. Hayashi and H. Imai, Chem. Commun., 2841–2843 (2007).
[21] F.C.M. Driessens and R.K. Verbeeck, Biominerals, CRC Press, Florida (1990).
[22] M. Tanahashi and T. Matsuda, J. Biomed. Mater. Res., 34, 305–315 (1997).
[23] R. Murugan, S. Mohan and A. Bigotto, J. Korean Phys. Soc., 32, 505–512 (1998).
[24] S. Dubinsky, G.S. Grader, G.E. Shter and M.S. Silverstein, Polym. Degrad. Stab., 86, 171–178 (2004).
[25] S. Kurata and K. Umemoto, J. Jpn. Soc. Dent. Mater. Devices, 11, 256–261 (1992).
[26] F.T. Wall and J.W. Drenan, J. Polym. Sci., 7, 83–88 (2003).
[27] S.V. Dorozhkin and M. Epple, Angew. Chem. Int. Ed., 41, 3130–3146 (2002).
[28] J.C. Heughebaert and G.H. Nancollas, J. Phys. Chem., 88, 2478–2481 (1984).